Supplementary Table 1: Demographics and clinical details of trauma patient population.

Sex	Age	Mechanism of Injury	Time to sample (min)	Head & Neck injuries	AIS	Face injuries	AIS	Chest injuries	AIS	Abdomen-Pelvic contents injuries	AIS	Extremity -Pelvic girdle bony injuries	AIS	ISS	Systolic BP (mmHg)	Serum buffer base Excess (U)
M	60	Motor vehicle crash	128	Scalp hematoma	1		0	Multiple rib fractures, flail chest, hemo-pneumothorax	4	Lumbar spine fracture	2	Pelvis and multiple arm fractures	3	29	121	-0.8
M	17	Motorcycle crash	129	Intracranial hemorrhage. Cerebral edema. Multiple skull and facial fractures	4	Multiple facial fractures.	2	Pneumothorax Pulmonary contusions	5		0	Wrist fracture, burn of calf	2	45	117	-8.2
M	41	Fall on to concrete	83		0		0	T12 spine fracture, rib fractures, bilateral hemothoraces	4		0	Pelvic and multiple upper & lower extremity fractures	5	41	64	-3.6
M	31	Pedestrian struck	76	Intracranial hemorhage. Skull fracture	5		0		0		0		0	25	132	-1.1
M	19	Motor vehicle crash	94	Diffuse brain injuries (DAI)	5	Facial fracture	2		0		0		0	29	124	2.9
M	59	Fall down stairs	89	Intracranial hemorrhage. Skull fracture.	4		0	Bilateral pulmonary contusions. Rib fractures	4		0	Fractured clavicle	2	36	128	-6.6
M	39	Fall down stairs	64	Intracranial hemorrhage. Skull fracture. Cerebral edema.	5		0	Pulmonary contusion. Rib fractures.	3		0		0	34	142	-0.8
M	51	Pedestrian struck	93	Intracranial hemorrhage. Diffuse brain injury (DAI)	4		0	T6, T8 spine fractures	3	Lumbar spine fracture	2	Multiple lower extremity fractures	3	34	71	-10
M	16	Motorcycle crash	87	Intracranial hemorrhage. Diffuse brain injury (DAI)	5		0		0		0		0	25	104	-1.2
M	27	Motorcycle crash	142		0	Multiple facial fractures	2	Multiple rib fractures, pulmonary contusions, hemopneumothorax, T3/4 spine fractures. Spinal cord injury.	5		0	Fractured scapula	2	33	84	-1.9
F	75	Pedestrian struck	75	Intracranial hemorrhage. Skull fracture.	4	Multiple facial fractures	0	Rib fractures, flail chest bilateral pneumo-thoraces and pulmonary contusions	4	Lumbar spine fractures	2	Multiple pelvis and upper extremity fractures.	3	43	128	-3.9
M	71	Motor vehicle crash	111	Cervical spine fracture dislocations. Spinal cord injury.	4		0	Rib fractures	1		0	Multiple upper extremity fractures	3	26	93	-0.3
F	66	Motor vehicle crash – ejected	98		0	Facial fracture	2	Rib fractures, pneumothorax	5		0	Fracture-dislocation left hip	2	33	134	3.1
F	59	Fall 4 floors	92		0		0		0	Abdominal hemorrhage	0	Pelvic fracture and retroperitoneal hemorrhage	5	25	unmeasurable	-8.7
M	17	Motorcycle crash	120	Intracranial hemorrhage. Diffuse brain injury (DAI)	5	Multiple face/ jaw fractures	3	Pneumothorax, T6 spine fracture	3		0	Pelvis and lower extremity fractures	2	43	144	-3.1

Trauma patients having serum mtDNA measurements (**Supplementary Figure 1)** had no significant medical co-morbidities, and no major open or intestinal injuries (study exclusions). Mean age was 43±21SD (median 41) years. Mean sampling time was 98±23SD (median 93) minutes. The AIS (Abbreviated Injury Score) was scored for each body region. Each injury or group of injuries is assigned 0-5 points. The ISS (Injury Severity Score) is the global sum of the three worst AIS scores squared (0-75 points). BP=blood pressure. Buffer base excess (calculated from arterial pH/pCO_2) indicates tissue perfusion.

Supplementary Table 2: Demographics of volunteer control blood donors

Sex	Age	Trauma or injury at time of sample	Acute diseases	Chronic diseases
M	28	None	None	None
F	62	None	None	None
F	30	None	None	None
M	56	None	None	None
M	54	None	None	Type II Diabetes
F	37	None	None	None
M	61	None	None	Type II Diabetes
M	32	None	None	None
F	38	None	None	None
M	33	None	None	None
F	34	None	None	None
M	26	None	None	None

Clinical data is presented for volunteer blood donors with serum mtDNA measurements shown in Supplementary Fig. 1. No patient had an acute injury. Two subjects had chronic uncomplicated type II diabetes. Mean age was 41±14SD (median 36) years.

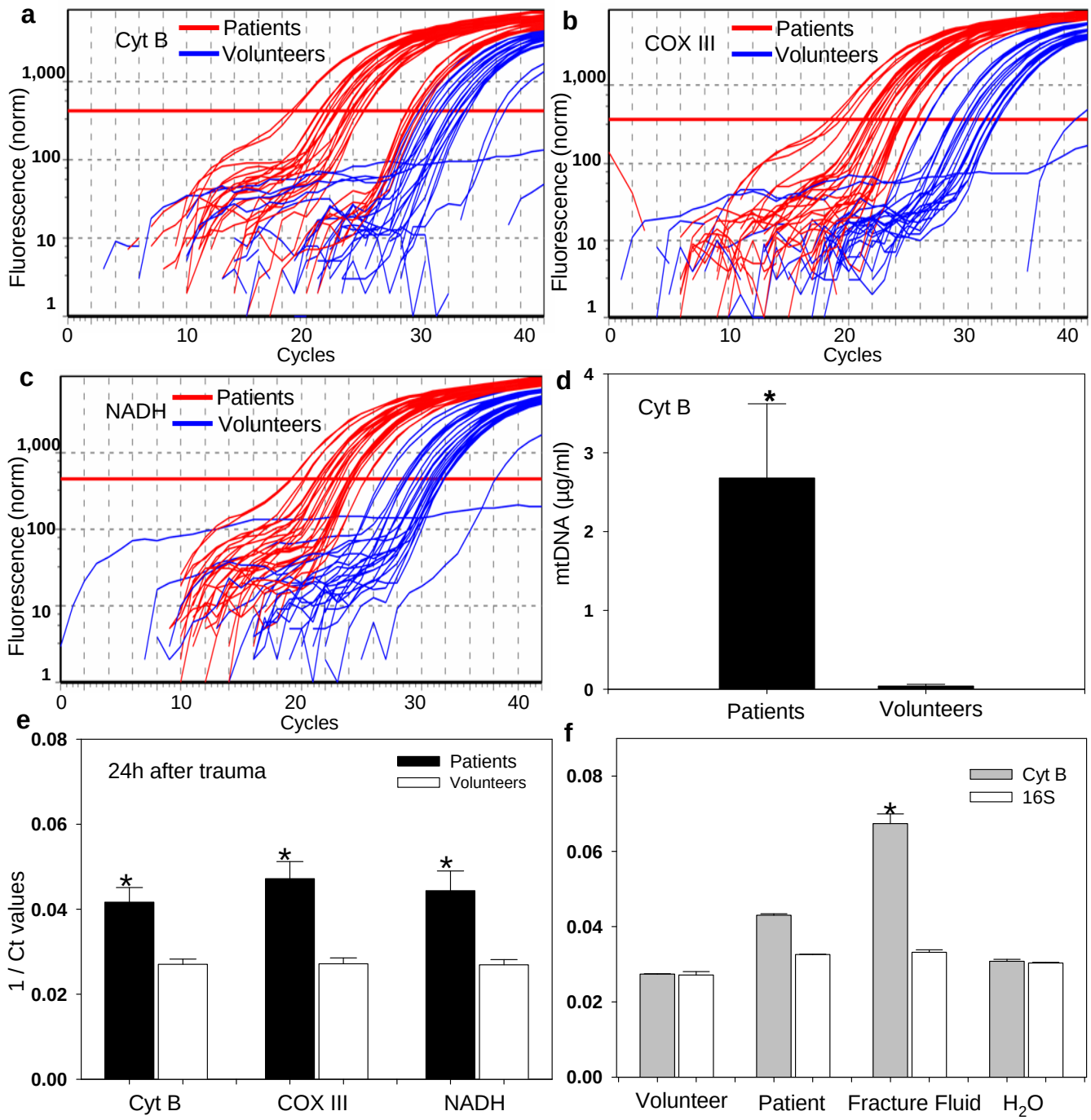

Supplementary Figure 1: **Clinical trauma results in circulation of mtDNA.** qPCR traces show that mtDNA is released in high concentration by injury **(a-c)**. Absolute Cyt B concentration is shown (**d)** in patients and volunteers (n=12, *p<0.05, *t*-test). mtDNA was sampled (**e)** in patient plasma 24h post-injury (n≥10, *p<0.01, *t*-test). 1/Ct denotes the reciprocal of the count where the sequence is detected: a direct function of concentration. mtDNA was assayed in supernatants of reaming fluids (**f)** from clinical fracture repairs (n≥10, *p<0.01, ANOVA/Dunn). qPCR for bacterial 16S rRNA showed no bacterial contamination of any specimen.

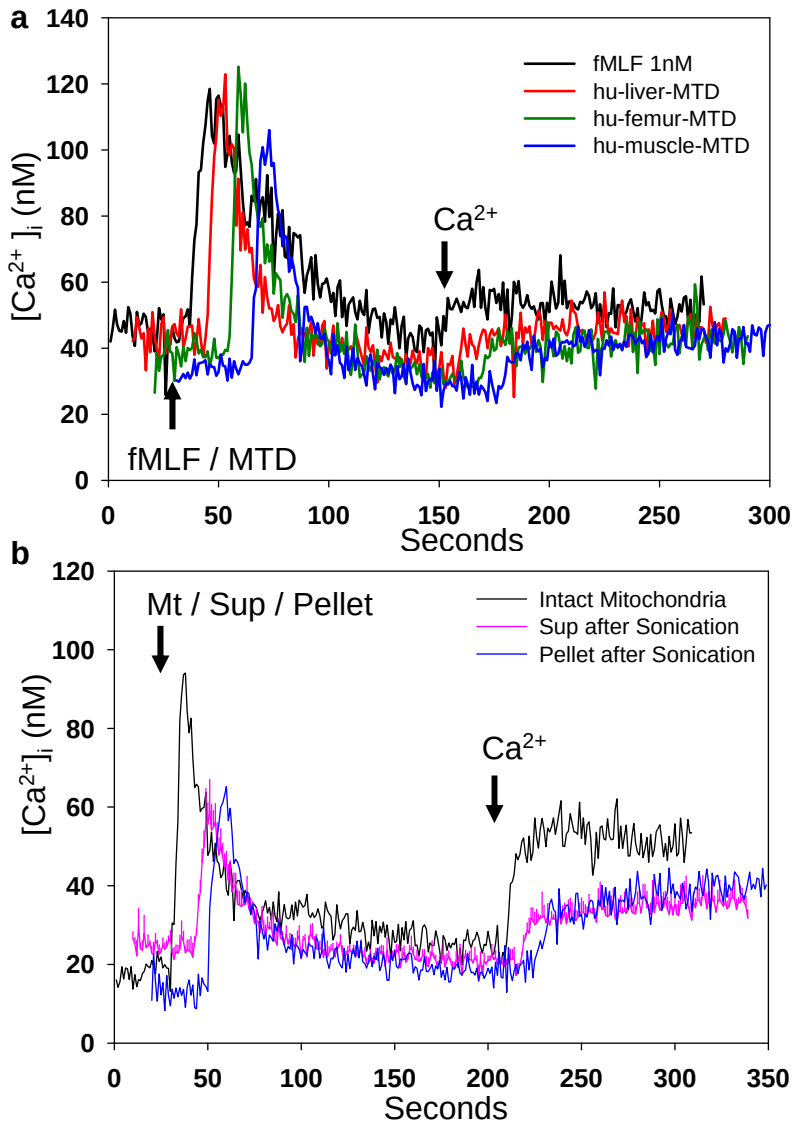

Supplementary Figure 2: Potency of MTD from differing sources
a. MTD derived from human liver, human femur fractures, and human skeletal muscle produce similar PMN calcium fluxes at the same dilutions, approximating the response to 1nM fMLF at ~1/100 dilution. **b.** The calcium response to intact mitochondria is approximately the sum of responses to the supernatants and pellets produced by sonication and centrifugation of mitochondria. All traces are the means of 3 experiments. Some traces are displaced for ease of viewing.

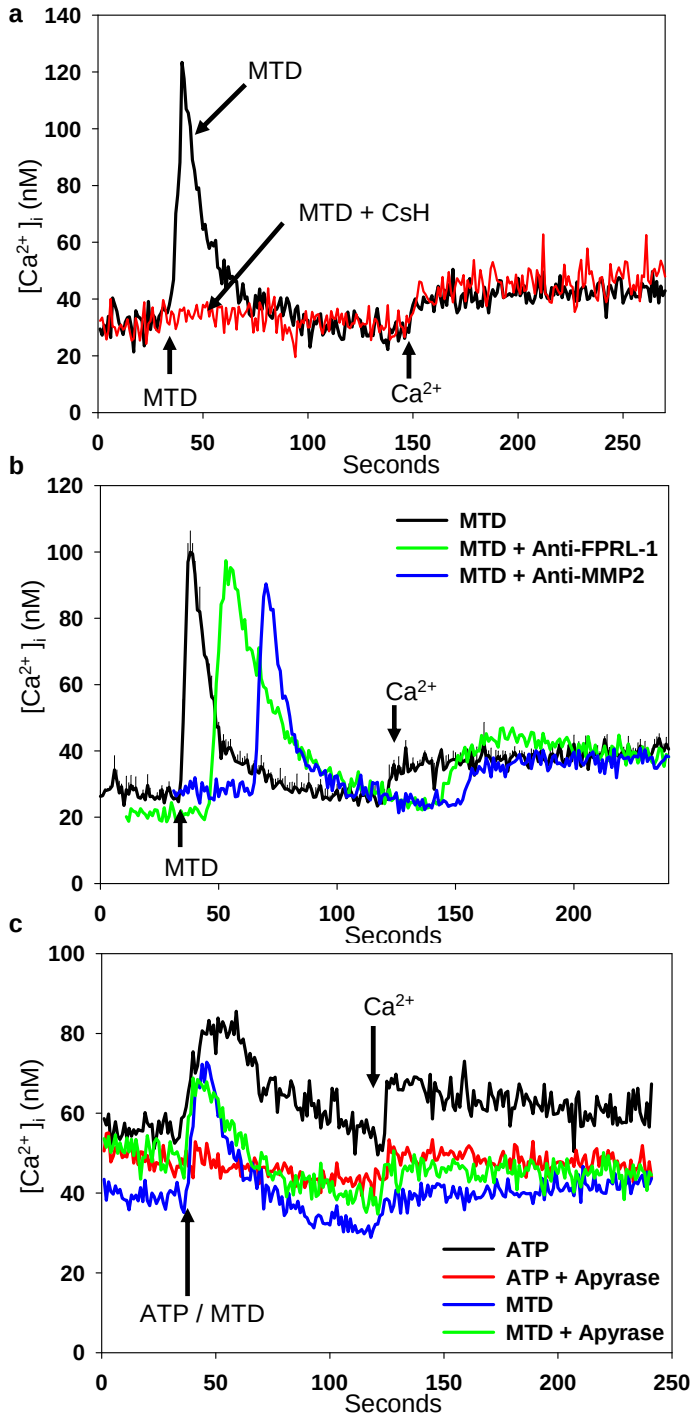

Supplementary Figure 3: MTD mobilizes $[Ca^{2+}]_i$

CsH specifically inhibits FPR-induced human PMN calcium depletion (**a**), and isotype control antibodies for that experiment (anti-FPRL-1, anti-MMP-2) have no effect on PMN responses to MTD (**b**). 1mM ATP mobilizes PMN $[Ca^{2+}]_i$ (**c**, black trace). Treatment of ATP with apyrase destroys ATP (**c**, red trace) and aborts Ca^{2+} signaling. MTD causes $[Ca^{2+}]_i$ signaling (**c**, blue trace) that is resistant to apyrase (**c**, green trace) showing MTD Ca^{2+} signaling is not due to ATP. Representative traces, displaced for ease of viewing.

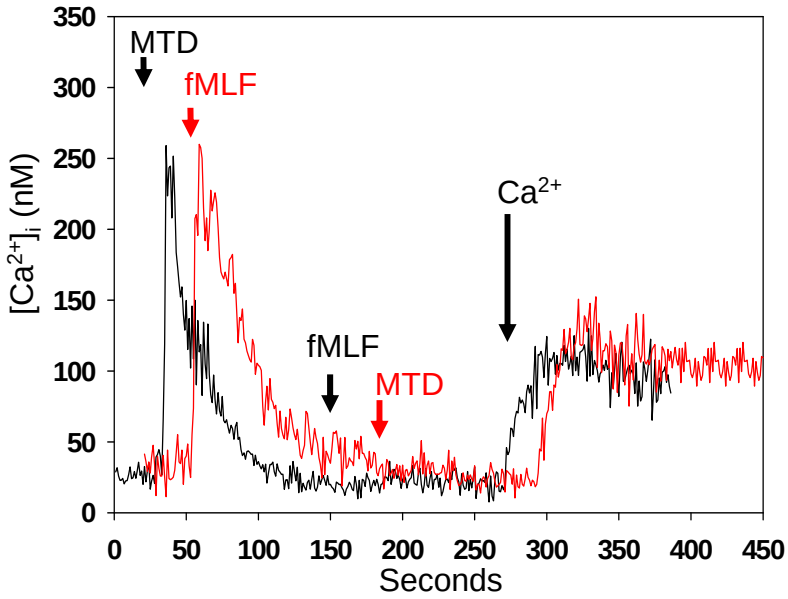

Supplementary Figure 4: MTD homologous desensitization
PMN treated with sequentially applied MTD-fMLF (black trace) or fMLF-MTD (red trace) showed completely inhibited Ca^{2+} responses to the second stimuli. All traces are means of 4 experiments, displaced for ease of viewing.

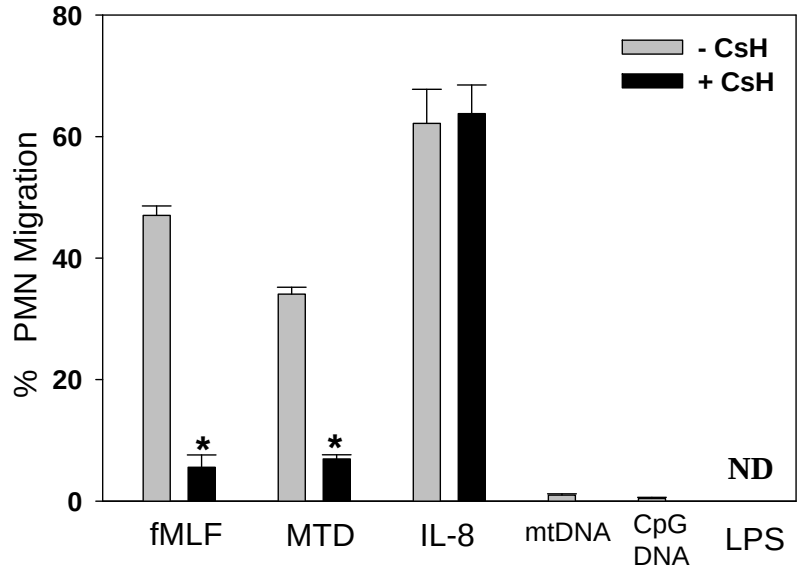

Supplementary Figure 5: PMN chemotaxis in transwell assay.
PMN show brisk chemotaxis to fMLF (10nM), MTD (100µg/ml) and IL-8 (10nM). CsH (1µM) significantly inhibits PMN migration to fMLF and MTD, but not to IL-8. PMNs show no primary chemotactic responses at all to the TLR agonists mtDNA (10µg/ml), CpG-DNA (10µg/ml), and LPS (1 µg/ml). n=3,*$p<0.05$ (*t*-test).

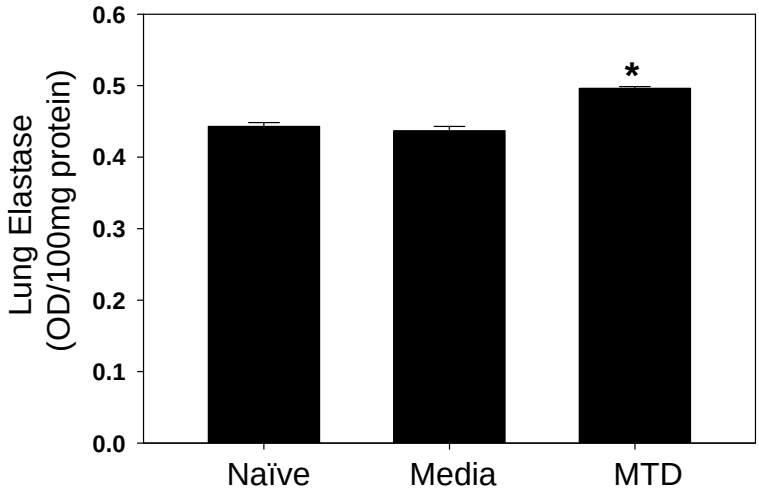

Supplementary Figure 6: PMN elastase in rat lung
Rats injected with MTD showed increased elastase levels in whole lung homogenates. ($n \geq 3$ for each group of rats, $^*p<0.05$, ANOVA/Holm-Sidak).

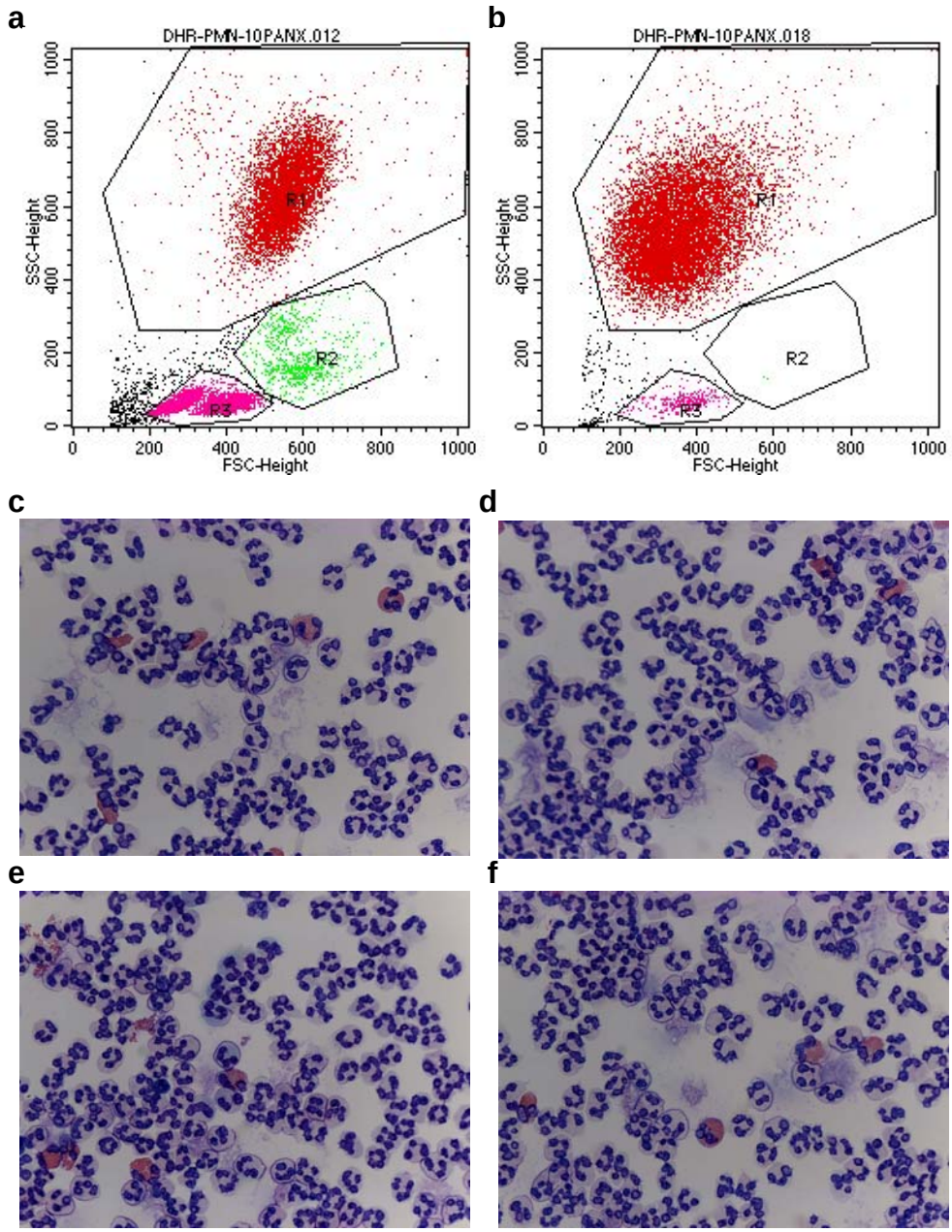

Supplementary Figure 7: PMN purity

PMN purity was confirmed by flow cytometry. Representative forward and side scatter dot plots show neutrophils in red (R1) and monocytes in green (R2). Whole blood with RBC lysis (**a**), R1= 53.2% and R2= 6.28%. PMN isolated from whole blood with RBC lysis (**b**), R1= 95.24% and R2= 0.02%. PMN purity was then confirmed by cytospin with HEMA-3 stain and visual inspection. Four random fields are displayed (**c**-**f**). Monocytes are absent.